Chemical Engineering Journal Advances 19 (2024) 100627

Contents lists available at ScienceDirect

Chemical Engineering Journal Advances

journal homepage: www.sciencedirect.com/journal/chemical-engineering-journal-advances

Exploring the role of hydrogen peroxide dosage strategies in the photo-Fenton process: Scaling from lab-scale to pilot plant solar reactor

Bárbara N. Giménez [a,b], Agustina V. Schenone [a,b], Leandro O. Conte [a,c,*]

[a] Instituto de Desarrollo Tecnológico para la Industria Química (INTEC), Consejo Nacional de Investigaciones Científicas y Técnicas (CONICET) and Universidad Nacional del Litoral (UNL), Ruta Nacional N° 168, 3000, Santa Fe, Argentina
[b] Facultad de Bioquímica y Ciencias Biológicas, Universidad Nacional del Litoral (UNL), Santa Fe, Argentina
[c] Facultad de Ingeniería y Ciencias Hídricas, Universidad Nacional del Litoral (UNL), Santa Fe, Argentina

ARTICLE INFO

Keywords:
Solar photo-Fenton
Pilot plant reactor
Ferrioxalate
Natural pH
Hydrogen peroxide dosage strategies
Pharmaceutical wastewater

ABSTRACT

This study aims to investigate the role of hydrogen peroxide (HP) continuous dosage in removing Paracetamol (PCT) from different water matrices using the solar photo-Fenton process. Different parameters in the HP dosage strategies (initial HP pulse, dosing time, and HP concentration) were systematically analysed to assess their impacts on pollutant removal (X_{PCT}), oxidant specific consumption ($Y^{t}_{HP/PCT}$), and toxicity levels (I(%)). The analysis involved various water matrices (ultrapure water UW, groundwater GW, anion matrix AW, and synthetic pharmaceutical wastewater IW0.01 or IW0.1), which were firstly treated in a laboratory reactor and subsequently scaled up to a solar prototype. After laboratory testing, the most effective reaction configuration (maximum X_{PCT} and $Y^{t}_{HP/PCT}$ close to the stoichiometric one) was chosen as the starting point for scaling up the reaction system. Using the solar reactor setup, complete PCT conversion was achieved within just 60 min of reaction time (UW matrix). However, under IW0.1 condition and employing the same HP dosing strategy, a X_{PCT} of 95.4 % was attained but at 180 min of reaction, highlighting the significant influence of the real matrix. Additionally, the I(%) remained high towards the end of the reaction (close to 60 %), attributed to the presence of hydroquinone in the system, demanding longer reaction times to completely reduce the toxicity when working with industrial wastewater. This comprehensive approach aims to close the gap between lab results and practical applications, offering crucial insights to address pharmaceutical wastewater pollution.

1. Introduction

The growing concern over Emerging Contaminants (ECs) is evident, particularly with substances such as pharmaceuticals and personal care products (PPCPs), pesticides, dyes, antibiotics, and antibiotic-resistant genes (ARGs) [1]. These pollutants have diverse sources, including industrial wastewater, domestic sewage, livestock and poultry wastewater, and hospital wastewater [2], having potential risks to both ecological environments and human health [3]. PPCPs have become pervasive in the environment due to their extensive production and use [4]. Specifically, substantial quantities of Paracetamol (PCT) were discharged into water systems because of its widespread use, inadequate disposal practices by manufacturers, limited metabolic breakdown in the human body, and their biologically active structures [5]. High concentrations of PCT (up to 300 mg L^{-1}, [6]) were detected in hospital effluents [7], pharmaceutical industry wastewater [8], and urban sewage treatment plants [9]. It is, therefore, unsurprising that pharmaceuticals are identified in receiving surface water [10], groundwater [11] and in some instances, even in drinking water [12].

The standard technologies implemented by wastewater treatment plants (WWTPs) are often ineffective in efficiently removing these contaminants of emerging concern [13]. Similarly, other water treatment methods such as reverse osmosis [14], and carbon adsorption [15], primarily shift these pharmaceutical pollutants from one phase to another but do not effectively remove them [16]. Advanced Oxidation Processes (AOPs), with a particular focus on the Fenton and photo-Fenton systems, have gained significant attention. These well-established and highly efficient technologies are widely utilized for treating both natural waters and wastewater. They exhibit the capability to eliminate a broad spectrum of contaminants, a task that conventional

* Corresponding author at: Instituto de Desarrollo Tecnológico para la Industria Química (INTEC), Consejo Nacional de Investigaciones Científicas y Técnicas (CONICET) and Universidad Nacional del Litoral (UNL), Ruta Nacional Nº 168, 3000, Santa Fe, Argentina.
E-mail address: lconte@santafe-conicet.gov.ar (L.O. Conte).

https://doi.org/10.1016/j.ceja.2024.100627

Available online 4 July 2024

treatment methods often find challenging to address [17].

The photo-Fenton process is a photocatalytic method that generates highly reactive hydroxyl radicals (HO•) by combining chemical reagents (Fe(II)/Fe(III) salt/complex and hydrogen peroxide, HP) with UV–Vis irradiation, resulting in a synergistic effect that accelerates the production of hydroxyl radicals. Nonetheless, there are significant limitations associated with this "traditional" process approach [18]. Firstly, the regeneration of Fe(II) from Fe(III) was identified as the step that limits the rate of the process. In this context, light plays a crucial role, serving as an "activator" for the regeneration of Fe(II) and, consequently, accelerates the overall reaction [19]. Here, the use of iron complexes proves to be advantageous, allowing operation at a neutral pH, preventing iron precipitation, and expanding the application range of the process to the visible region of the solar spectrum [20]. Giménez et al. [21] have already demonstrated the feasibility of the Ferrioxalate-assisted Photo-Fenton Process (Fe-Ox-PFP) applied to the degradation of Paracetamol (PCT). Secondly, hydroxyl radicals are highly unstable and non-selective, making them prone to unwanted secondary reactions, some of which involve HP consumption, reducing the process efficiency [22]. Moreover, an oversupply of hydrogen peroxide can undergo spontaneous decomposition into oxygen and water [23]. Consequently, it is crucial to control the reaction conditions by adjusting the oxidant dosage, which is frequently the most costly reagent, to achieve the complete degradation of the target compound [24]. Then, a balance between the low decontamination efficiency of the process, caused by insufficient hydrogen peroxide dosage, and the additional expenses linked to an excess of it, need to be established. To address this issue, researchers have explored the use of different HP dosage strategies to enhance the performance of the photo-Fenton process [24–26].

In recent years, solar technology has transformed the photo-Fenton process into a cost-effective and competitive method for chemical degradation of organic pollutants. Solar reactors offer an intriguing alternative for effluent treatment, eliminating expenses associated with UV lamps installation and maintenance, and reducing electrical power consumption [27]. The literature specifically highlights the application of the solar photo-Fenton process in remediating water containing ECs, including PPCPs [28], pesticides [29], dyes [30], antibiotic [31], ARGs [32], effluents from municipal treatment plants [33] and hospitals [34]. However, cost considerations, particularly regarding the oxidizing agent, are important to address. In systems operating at natural pH and utilizing solar radiation, the oxidizing agent can be one of the most expensive reagents [35]. The pursuit of automating the photo-Fenton process is driven by the goal of improving its performance, with a focus on decreasing hydrogen peroxide consumption compared to manual operation. This objective is directed at lowering both the economic cost and process time, ultimately enhancing resource use efficiency.

It is important to highlight that a considerable number of scientific articles focus only on studying the degradative behaviour of PPCPs in ideal water matrices. However, in real aqueous environments, a range of substances may coexist, posing potential obstacles to the breakdown of these contaminants via the photo-Fenton process. Anions (chlorides, nitrates, bicarbonates, and sulphates) are recognized for interfering in the reaction, as they act as scavengers for the HO• produced [36]. Cations (mainly, calcium and magnesium) can interfere with the Fe (III)/Oxalate equilibrium/precipitation reactions, affecting the photochemical activity of the system [37]. The influence of both cations and anions is crucial because, in many industrial pharmaceutical plants, the water supply for cleaning the reactors comes from underground wells. Furthermore, in real pharmaceutical industry effluents, many agents (such as detergents), are employed to clean the formulation reactors. Thus, all these interferences contribute to a reduction in the pollutants degradation rates and an increase in the HP consumption [38,39]. Giménez et al. [40] assessed a straightforward and punctual HP dosing strategy within a laboratory-scale reactor across various complex water matrices using the Fe-Ox-PFP. Unlike many studies that typically focus on PPCPs degradation under controlled conditions, this research emphasized the effectiveness of HP dosage in enhancing the iron catalytic cycle. The results showed substantial improvements in both Fenton and photo-Fenton reactions, indicating promising applications despite the limitations of the experimental scale.

Indeed, the assessment of purification technologies like the photo-Fenton process in real-world scenarios is crucial for addressing the challenges posed by persistent contaminants in complex effluents. In this context, the current research aims to address the removal of Paracetamol (PCT) from complex pharmaceutical wastewater effluent. The chosen approach involves harnessing the solar photo-Fenton reaction, operating at a near-neutral pH and incorporating oxalate as a complexing agent to form ferrioxalate. A fundamental aspect of this research lies in investigating different parameters in the HP dosage strategies (initial HP pulse, dosing time, and HP concentration), which play vital roles in determining the efficiency of the Fe-Ox-PFP in the removal of PCT present in a simulated pharmaceutical wastewater employing a real pilot plant solar reactor, including considerations regarding toxicity levels. Through systematic experimentation and analysis, the research aims to optimize the dosing strategy to maximize pollutant removal while minimizing operational costs and environmental impacts.

2. Material and methods

2.1. Experimental devices

In this investigation the experiments were conducted employing two different photoreactors. The first one was a batch lab-scale reactor irradiated by a solar simulator. This unit operates under perfect mixing conditions and at a constant temperature. Details of this experimental system can be referenced elsewhere [41]. Here, the local radiation flux averaged over the reactor window (q_W) was 92.80 W m^{-2} (32.2 nE cm^{-2} s^{-1}), within the wavelength range of 300 to 500 nm (USB spectrometer, Ocean Optics, USB2000). This radiation level simulates the annual average natural radiation condition frequently found in the city of Santa Fe (Argentina, 31° 39′ S, 60° 43′ W, 25 m above sea level). The total volume of the treated solution was 3 L.

The second reactor utilized in this study was a pilot-plant non-concentrating solar photoreactor, specifically designed to capture UV/visible and near-infrared solar radiation (patent INPI P-080103697). The entire reaction system operates within a closed recirculating circuit, which is facilitated by a high flow rate centrifugal pump and a well-stirred storage tank. The storage tank is equipped with a pH-meter and an OD sensor from HANNA Instruments. Additionally, type J thermocouples are employed to monitor temperature variations at different positions in the system over time. To measure the UV and total broadband solar radiation fluxes incident on the two-plate reactor window, CUV3 and CM11 Kipp and Zonen radiometers were employed. The irradiated reactor volume was 6.1 L, while the total volume of the treated solution was 35 L. For further detailed information regarding this solar photoreactor, please refer to [29]. Finally, both experimental setups (laboratory and pilot plant units) were equipped with a diaphragm dosing pump (Acquatron® MA-CP series) for the automatic addition of the oxidizing agent.

2.2. Analytical determinations

Paracetamol (Sigma-Aldrich, 98 % purity) served as the model pollutant. The concentrations of PCT and its main reaction intermediate, hydroquinone (HQ) (Fluka, 99 % purity), were analysed by HPLC-DAD (Waters) following the methodology outlined in Giménez et al. [21]. The mineralization achieved was monitored via TOC measurements employing a Vario TOC cube analyzer (Elementar). Hydrogen peroxide (Cicarrelli, 30 %) and total iron were determined using a UV/Vis spectrophotometer (Lambda 35, Perkin-Elmer). For HP, a modified

iodometric technique was applied (measurement at 350 nm). Both the samples for total Fe (pre-treated with ascorbic acid) and Fe^{2+} were analysed using the colorimetric method with 1,10-phenanthroline at 510 nm [41]. Finally, the oxalate ion (Oxa) was quantified by an ion chromatography-conductivity detector (Waters) with an IonPac AS22 anion exchange column and an IonPac AG22 guard column (Dionex). The eluent consisted of 4.5 mM Na_2CO_3/1.4 mM NaOH (flow rate of 1.2 mL min^{-1}). For the preparation of the ferrioxalate complex, a solution of potassium oxalate monohydrate (Carlo Erba, 99.5 %) and a solution of iron(III) chloride were mixed in appropriate proportions. Ultrapure water was obtained using a reverse osmosis system (Osmoion, APEMA).

A Microtox Model 500 Toxicity Analyser (Strategic Diagnostic Inc.) was utilized to assess acute toxicity of the samples throughout the oxidation process. Toxicity was computed as the percentage of light emission inhibition by the *Vibrio fischeri* NRRL-B-11177 bacteria following a 15-minute incubation period. Light inhibition measurements were conducted without sample dilution. Prior to toxicity assessments, sample pH was adjusted within the range of 6 to 7 and any residual hydrogen peroxide in the aqueous sample was decomposed into water and oxygen using a catalase solution (1500 mg L^{-1} of >2000 U/mg bovine liver, Fluka)

2.3. Experimental procedure

For the tests conducted in the pilot plant solar reactor, each experimental assay began with the introduction of PCT and ferrioxalate solutions into the storage tank of the system. At the beginning of these experiments, a solar-opaque plate protected the reactor window to prevent solar radiation entry. In all cases, the medium pH was adjusted to 5 using either a concentrated sodium hydroxide solution (3 mol L^{-1}, Cicarelli) or sulphuric acid (3 mol L^{-1}, Cicarelli), depending on the initial pH of the solution under treatment. The oxidizing agent was added according to the evaluated dosing strategy, and upon addition, the first sample was taken, and the reactor cover was removed to initiate the photochemical reaction. The solar experiments began at 10.0 LST and the reaction progress was monitored over 180 min, taking samples at predefined times for various analyses and parameter assessments. An analogous procedure was performed when operating the laboratory-scale reactor, although a constant temperature of 25 °C was maintained throughout the reaction time, in order to avoid inefficient use of hydrogen peroxide at higher temperatures. More details of the experimental procedure can be found in [29].

To determine the oxidant concentrations for dosing, the stoichiometric quantity necessary to achieve complete mineralization was calculated assuming HP as the sole oxidant in the medium and PCT concentration at 40 mg L^{-1}. The calculated value was 189 mg L^{-1}. Then, a range between a quarter and four times the stoichiometric dose (47.25 and 756 mg L^{-1}, respectively) was chosen. Moreover, selecting doses higher than the stoichiometric value (189 mg L^{-1}) is based on the demonstrated improvement in conversion levels within shorter reaction times [18].

Specifically, regarding the dosage of HP, two strategies were evaluated: 1) starting with an initial pulse of reagent, followed by a continuous additional dosage of HP until 75 or 150 min of reaction; 2) beginning the test without an initial pulse of reagent, instead, starting with a continuous dosage of the oxidizing agent until 75 or 150 min of reaction (see Table 1 and Table 2).

Finally, the treated samples consisted of: a) ultrapure water (UW), b) an artificial matrix of anions in ultrapure water (AW), c) real groundwater (GW) and d) synthetic industrial wastewater coming from a pharmaceutical plant (IW0.01 or IW0.1). In all the experiments, initial PCT, Oxa, and Fe concentrations were set at 40 mg L^{-1}, 47.5 mg L^{-1}, and 3 mg L^{-1}, respectively. The initial concentration of PCT was determined based on observed levels in actual pharmaceutical industry wastewater [6,42]. For iron, the concentration was selected in accordance with legal discharge limits for treated effluent into surface water bodies, set at 5 mg L^{-1} [43]. To achieve a molar ratio of Fe/Ox=1/10, the initial oxalate concentration was established at 47.5 mg L^{-1}, thereby preventing iron precipitation at the operational pH. Previous studies have shown that under these conditions, approximately 90 % of the ferrioxalate species present is the highly active $Fe^{3+}(C_2O_4)_3^{3-}$, which possesses significant molar absorption coefficients in the UV/Vis spectrum [41].

In the case of UW, AW, and GW, a PCT standard drug was added to obtain 40 mg L^{-1} in the total reaction volume (3 L). The AW matrix was prepared so that the final concentrations of each anion in the reaction volume were: 80, 50, and 100 mg L^{-1}, for Cl^-, SO_4^{2-}, and HCO_3^-, respectively. For this, NaCl, Na_2SO_4, and $NaHCO_3$ obtained from Cicarelli were used. The main characteristics of the GW sample and its composition can be found elsewhere [40].

For the synthetic industrial effluent, the source of PCT was a commercial pill (LIF, Cert. ANMAT Nº 54.235), containing pre-gelatinized starch, stearic acid, and povidone K30 as excipients. The effluent preparation involved the following steps. First, five commercial pills (each containing 500 mg of paracetamol) were weighed and pulverized. The mass equivalent to one pill was dissolved in 500 mL of ultrapure water, resulting in a solution of 1 g PCT L^{-1}. Subsequently, 120 mL of the concentrated commercial PCT solution was added to achieve a final concentration of 40 mg L^{-1} of PCT in the total reaction volume (with TOC = 30.54 mgC L^{-1} for the diluted drug solution). Finally, CIP300® (a neutral pH detergent commonly used in the pharmaceutical industry) was added at a concentration of 0.01 % (IW0.01) or 0.1 % (IW0.1) in the system (TOC = 54.74 mgC L^{-1} for a solution of CIP 0.1 %), contributing to a total carbon amount of 85.28 mgC L^{-1} in the simulated effluent when using the 0.1 % CIP solution.

Table 1
Experimental conditions and PCT conversion (X_{PCT}^{180} (%)) after 180 min of reaction for lab-scale reactor.

Run	ID	HP (mg L^{-1})	Dosing time (min)	Rad[b]	Matrix[a]	Flow (mgHP min^{-1})	X_{PCT}^{180}(%)
N1*	378_IP_150_OFF_UW	378	150	OFF	UW	8.41	3.5
N2	47.25_NP_75_ON_UW	47.25	75	ON	UW	2.13	96.0
N3	94.5_NP _75_ON_UW	94.5	75	ON	UW	4.81	94.3
N4*	189_IP_150_ON_UW	189	150	ON	UW	3.61	93.3
N5	189_NP _150_ON_UW	189	150	ON	UW	4.81	93.9
N6*	378_IP_150_ON_UW	378	150	ON	UW	8.41	90.7
N7	378_NP _75_ON_UW	378	75	ON	UW	14.88	85.9
N8*	378_IP_75_ON_UW	378	75	ON	UW	16.63	87.8
N9	756_NP _75_ON_UW	756	75	ON	UW	34.03	79.0
N10	378_NP _75_ON_GW	378	75	ON	GW	16.63	99.5
N11	189_NP _75_ON_AW	189	75	ON	AW	8.51	97.7
N12	378_NP _75_ON_IW	378	75	ON	IW0.1	16.63	18.9

[a] UW: ultrapure water; GW: ground water; AW: artificial anion matrix; IW0.1: simulated industrial wastewater with 0.1 % CIP300.
[b] Rad = Radiation. ON: $q_W = 92.80$ W m^{-2}; OFF: without radiation.
* Runs with an asterisk are those that were carried out with an Initial Pulse (IP) of HP = 47.25 mg L^{-1}.

Table 2
Experimental conditions in the pilot plant solar reactor.

Run	HP (mg L^{-1})	T^{t0}(°C)	T^{t180} (°C)	Accumulated energy[a] (KJ L^{-1})	Flow (mgHP min^{-1})	Matrix[b]	X_{PCT} [c] (%)
S1	47.25	23.8	38.9	5.23E+04	21.88	UW	98.90 (60 min)
S2	378	25.8	35.9	2.50E+04	175	UW	98.70 (60 min)
S3	756	26.2	41.9	4.97E+04	350	UW	98.90 (45 min)
S4	378	28.0	39.9	3.35E+04	175	IW0.01	97.90 (60 min)
S5	378	29.0	44.2	4.02E+04	175	IW0.1	95.40 (180 min)

[a] Calculated at 180 min reaction time.
[b] UW: ultrapure water; IW0.01: simulated industrial wastewater with 0.01 % CIP300; IW0.1: simulated industrial wastewater with 0.1 % CIP300.
[c] Between parenthesis: time (min) at which the conversion value was reached.

3. Results and discussion

Two different photoreactors were utilized in this study: a batch lab-scale and a pilot plant solar reactor. These reactors were employed to assess the scalability and efficiency of hydrogen peroxide dosage in PCT photo-Fenton degradation.

3.1. Lab-scale reactor

Table 1 lists the set of experiments carried out in the lab-scale reactor in different matrices. The identification code (ID) used to describe each experimental condition includes: the theoretical target/final oxidizing agent concentration reached ("HP": 47.25, 94.5, 189, 378 or 756 mg L^{-1}), the addition of an initial punctual dosage of oxidant ("Initial Pulse": IP, initial pulse; or NP, no initial pulse), the period during which the oxidizing agent was added ("Dosing Time": 75, or 150 min); the radiation condition ("Rad": ON, or OFF), and the water matrix treated ("Matrix": UW, GW, AW and IW0.1). Thus, as an example, Run N1, ID:378_IP_150_OFF involves a final oxidant concentration of 378 mg L^{-1} (HP), an initial pulse of oxidizing agent (IP), oxidant dosing time of 150 min (Dosing Time), and non-irradiated reaction conditions (Rad).

The influence of radiation on the system is significant. Under dark conditions, using UW matrix (Run N1), PCT conversion only reached 3.5 % after 180 min of reaction. In contrast, a minimum conversion of 79.0 % was obtained under irradiated conditions (Fig. 1d, Run N9), where an excess of oxidizing agent was present in the system. Moreover, when radiation was applied, even at the lowest final concentrations of oxidizing agent (Fig 1c, HP = 47.5 mg L^{-1}, Run N2, and HP = 94.5 mg L^{-1}, Run N3), high PCT conversions were still achieved (greater than 94 %).

In second place, it can be observed that the influence of the initial pulse of HP was not significant in the achieved contaminant conversion levels (Fig. 1c, Run N4 vs. Run N5, and Fig. 1d, Run N7 vs. Run N8). There were also no substantial differences between contaminant conversion for a dosing time of 75 min (Run N7) vs. 150 min (Run N6). However, the main operational differences were found in the observed oxidizing agent consumption ($Y^{t}_{HP/PCT}$). At this point, the specific consumption of HP was defined as the difference between the mass of HP added to the reaction medium (HP^{t}_{dosed}) and the mass of HP quantified experimentally in the system ($HP^{t}_{measured}$), as a function of the mass of

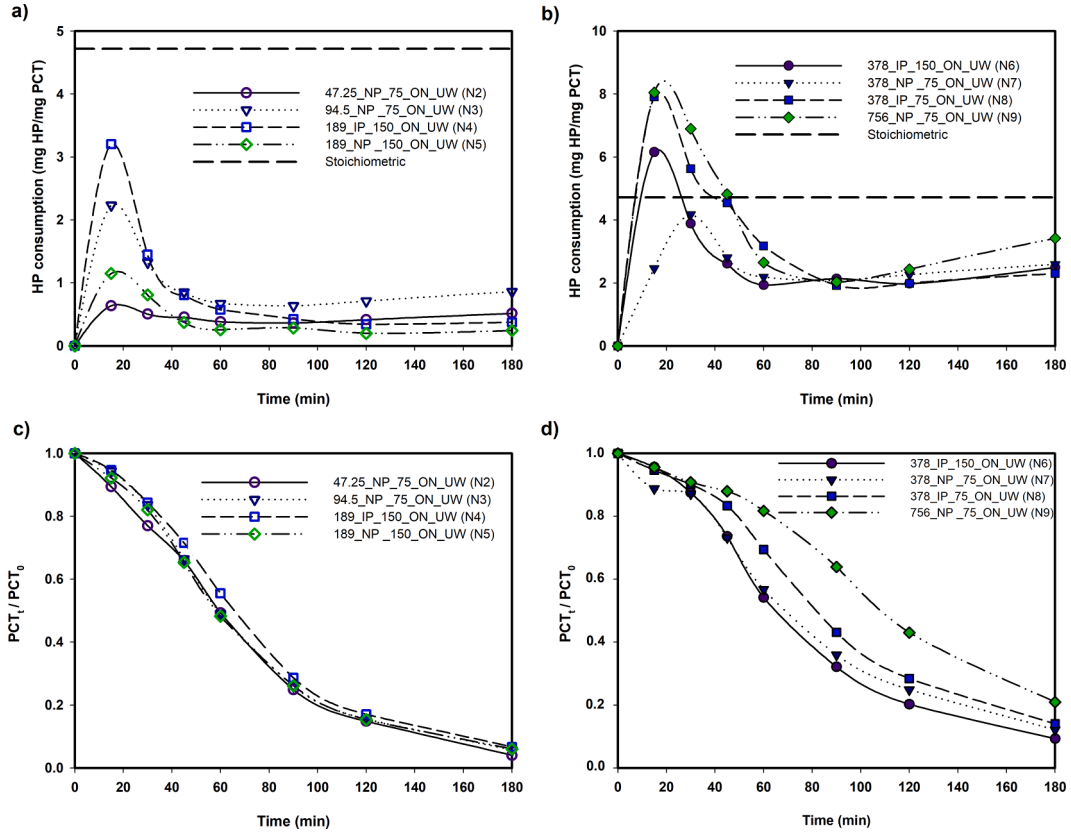

Fig. 1. Specific consumption of hydrogen peroxide for a) low HP concentrations (Runs N2 - N5) and b) medium and high HP concentrations (Runs N6 - N9); c) relative PCT concentrations for low HP conditions (Runs N2 - N5); d) relative PCT concentrations for medium and high HP concentrations (Runs N6 - N9).

PCT converted (Eq. (1), [41]).

$$Y^{t}_{HP/PCT} = \frac{\sum_{0}^{t}\left(HP^{t}_{dosed} - HP^{t}_{measured}\right)}{PCT^{0} - PCT^{t}} \quad (1)$$

The specific consumptions of oxidizing agent and PCT evolution are depicted in Fig. 1. For low doses of hydrogen peroxide (Fig. 1a, Runs N2 to N5), regardless of the reagent dosing rate used (75 or 150 min), the consumption of oxidizing agent remained below the stoichiometric value required for the mineralization of PCT (4.72 mgHP mgPCT^{-1}, Eq. (2)). Considering that a consumption value close to the stoichiometric one is associated with the complete removal of reaction intermediates, the studied dosing conditions were not sufficient to degrade the generated by-products [44].

$$C_8H_9NO_2 + 21H_2O_2 \rightarrow 8CO_2 + 25H_2O + H^+ + NO_3^- \quad (2)$$

In the case of medium and high HP doses (Fig. 1b, Runs N6 to N9), variable levels of oxidizing agent consumption were observed. Using maximum HP concentrations and HP dosage rates (Run N9), the specific unproductive consumption reached its maximum value (8.05 mgHP mgPCT^{-1} for 15 min of reaction). This excess of HP, besides interfering in the PCT degradation process, leads to excessive and nonspecific consumption of the oxidizing agent itself. This phenomenon arises from the reaction of HP with HO• radicals (Eq. (3)) or the self-decomposition of HP (Eq. (4)) [40]. However, for medium HP concentrations and dosage rates (Runs N6 and N7), this unproductive consumption decreased. In the conditions of Run N7, this value was close to the stoichiometric one (4.72 mgHP mgPCT^{-1}).

$$H_2O_2 + HO^{\cdot} \rightarrow HO_2^{\cdot} + H_2O \quad (3)$$

$$2H_2O_2 \rightarrow 2H_2O + O_2 \quad (4)$$

Based on these results, the conditions of Run N7 (continuous addition of HP until 75 min of reaction without initial punctual dosage) will be considered as the starting point for experiments with more complex matrices (Runs N10 to N12). PCT temporal evolution and calculated HP consumptions can be analysed in Fig. 2. In the case of AW and GW matrices, although high conversion levels of the pharmaceutical were achieved (Fig. 2c), the oxidizing agent consumptions were lower than the stoichiometric amount (Fig. 2a), indicating the formation of reaction intermediates [44]. Conversely, when evaluating synthetic industrial wastewater, PCT was poorly degraded (Fig. 2c, 18.9 % at 180 min) and the specific consumption was much greater than 4.72 mg HP mg PCT^{-1}, demonstrating a high unproductive consumption of the oxidant (Fig. 2b). Both effects can be associated with the contribution of organic matter to the reaction medium due to the components of CIP300® and the excipients in the pills of PCT. Furthermore, even though the composition of the detergent is not informed, it is known that anionic surfactants can form complexes with Fe ions, interfering with the catalytic cycle and the performance of the process [45].

For all the tests conducted in the laboratory reactor, the temporal evolutions of the catalyst (Fe^{+3}/Fe^{+2}) and the complexing agent (oxalate ion) were analysed. The maximum recorded oxalate conversion at 180 min was X^{180}_{OXA}= 19.69%, under the conditions of test N9 (using the maximum concentration of the oxidising agent, HP= 756 mg L^{-1}). However, no catalyst (Fe) precipitation was observed in any of the laboratory tests.

Regarding TOC analysis, the highest conversions achieved were observed in Run N6 (378_IP_150_ON_UW), reaching a maximum of X^{180}_{TOC}= 20.15%. Conversely, the lowest values were recorded in the case of simulated industrial wastewater in Run N12 (0.1 % CIP300), with X^{180}_{TOC}= 1.3%. Furthermore, for the conditions of tests N10 (GW) and N11 (AW), the X^{180}_{TOC} were less than 14%.

3.2. Pilot plant solar reactor

Table 2 presents the operating conditions of the runs performed in the solar reactor. The temperature increment, the total accumulated energy (between 300 and 550 nm), and PCT conversions were monitored for 180 min of reaction. For all the tests carried out, the dosing time of the oxidizing agent was set at 75 min and no initial HP pulse was employed. These conditions were defined considering the preliminary results obtained in the laboratory reactor.

Firstly, it's important to note that for each of the tests outlined in

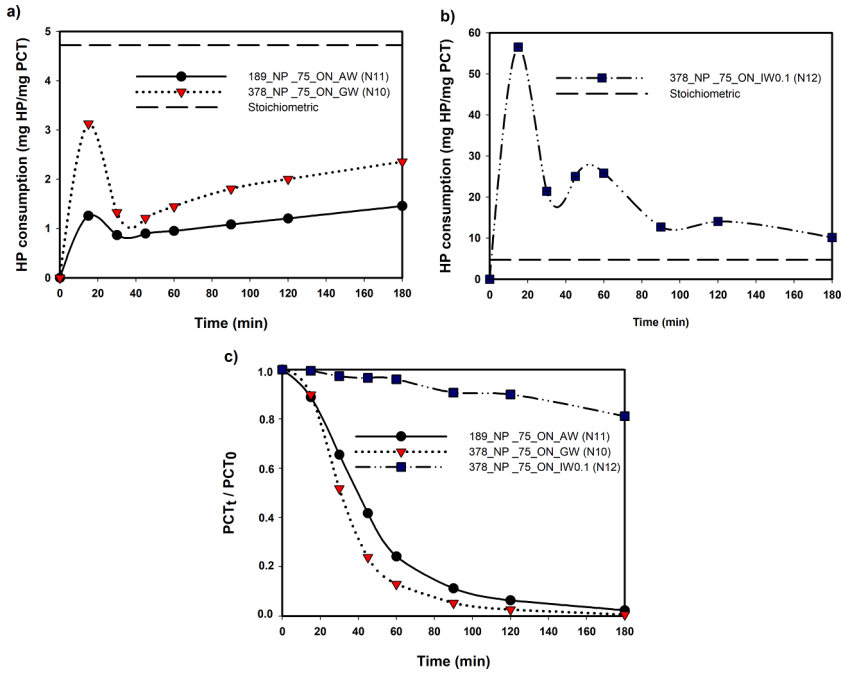

Fig. 2. a) and b) Specific consumption of hydrogen peroxide and c) relative PCT concentrations for complex matrices in the lab-scale reactor. GW: groundwater (Run N10, HP = 378 mg L^{-1}); AW: artificial anion matrix (Run N11, HP = 189 mg L^{-1}); IW0.1: simulated industrial wastewater with 0.1 % CIP300 (Run N13, HP = 378 mg L^{-1}).

Table 2 (Runs S1 to S5), variable values of accumulated energy and temperature increase were recorded due to the environmental conditions encountered during each experimental test. Therefore, the accumulated radiation ($Q_{300-550nm,\ t}$, KJ L^{-1}) in each experiment with solar radiation was calculated according to Eq. (5), [46]:

$$Q_{300-550nm,\ t} = Q_{300-550nm,\ t-1} + \Delta t_t \overline{RAD}_{300-550nm,t} \frac{A_r}{V_t} \quad (5)$$

where $Q_{300-550nm,\ t}$ is the total accumulated radiation (KJ L^{-1}), Δt represents the time interval (s), $\overline{RAD}_{300-550nm,t}$ is the average total radiation (W m^{-2}), A_r is the irradiated area (0.24 m^2), and V_t is the total volume of treated wastewater (35 L). The accumulated radiation was calculated between 300 and 550 nm, considering the photochemical characteristics of the employed ferrioxalate complex [47], which enables the utilization of both, UV and visible radiation. Therefore, this accumulated radiation represents the energy required for the photochemical activation of the process.

Fig. 3 shows the evolutions associated with PCT degradation, as a function of accumulated energy.

The results presented in Table 2 and Fig. 3 illustrate the efficacy of the examined process. First, complete conversion of PCT was attained within just 60 min of reaction (Runs S1 to S3) for UW conditions. However, when employing low doses of oxidizing agent (Run S1), a notable decrease in the rate of contaminant degradation was evident. In fact, up to 200 % more accumulated energy was needed (5.23×10^4 KJ L^{-1} vs. 2.50×10^4 KJ L^{-1}) to achieve complete conversion of the contaminant compared to an intermediate oxidant concentration of 378 mg L^{-1} (Run S2). Finally, dosing an excess of HP (Run S3) did not lead to any benefit in the degree of PCT degradation.

It is noteworthy to emphasize the effectiveness of the investigated process even under conditions that simulate an industrial effluent (IW0.01 and IW0.1). Remarkably high contaminant conversions (up to 98 %) were achieved within just 60 min of reaction for low detergent concentrations (Run S4, IW0.01). However, when a higher detergent percentage was introduced under the same HP level (Run S5, IW0.1), a conversion of 95.4 % was attained but at 180 min, indicating the significant influence of the real matrix (and consequent consumption of hydroxyl radicals). It's important to note that despite using the same hydrogen peroxide (HP) concentration (378 mg L^{-1}) and dosing strategy, the combined effect of UV/visible and thermal sunlight was able to almost completely degrade PCT after 180 min of reaction in the simulated industrial wastewater (Run S5). This contrasts with the conversion value of 18.9 % achieved in the lab-scale reactor (Run N12, Table 1).

For all tests conducted in the solar reactor, the maximum recorded oxalate conversion was $X_{OXA}^{180} = 74.53\%$, under the conditions of test S3 (using the maximum concentration of the oxidising agent, HP= 756 mg L^{-1}). Unlike the laboratory tests, in this case, a maximum final precipitation of the catalyst close to 75 % was observed.

Dissolved oxygen (DO) profiles were monitored throughout the reaction as an easily quantifiable variable associated with the evolution of the photo-Fenton process and its efficiency [48]. Fig. 4a illustrates the evolution of DO as a function of accumulated energy for Runs S1 (HP deficit) and S3 (HP excess). Under the conditions of run S1, a constant decay in the DO concentration was observed (up to 40 % of the saturation value of 7.10 mg L^{-1}) during the progress of the reaction. This observation suggests a Dorfman-type mechanism in the system, where dissolved oxygen actively participates in the oxidative process [23].

However, using an excess of oxidizing agent (Run S3), two distinct behaviours were observed in the evolution of the DO. Initially, for low reaction times, the amount of the oxidizing agent (Fig. 4b) was insufficient. Considering the high initial reaction rate of the system, a DO consumption of up to 75 % of the saturation value was reached. In a subsequent stage, hydrogen peroxide accumulated in the system and began to be in excess (up to 250 mg L^{-1}). At this point, it initiated parallel reactions, such as self-decomposition and reaction with free radicals, resulting in the production of O_2 and subsequent increase in the DO profile up to 130 % of the saturation value (Eq. (3) and Eq. (4)) [26].

Analysing the achieved TOC conversion is crucial for assessing the overall effectiveness of the degradation process. In the case of pure water samples (Runs S1-S3), the relative TOC concentration (Fig. 5) values obtained at 180 min ranged between 32.7 % and 38.7 % (corresponding to conversions between 61.3 % and 67.3 %). However, an analysis of the system mineralization as a function of accumulated energy reveals that the presence of detergent and the drug excipients (Run S4 and S5) negatively affected the rate and final conversion of TOC (Fig. 5), only reaching 10 % mineralization for the conditions of Run S5 (IW0.1). Indeed, the performance of the photo-Fenton process in the solar pilot plant device surpassed that observed in the laboratory-scale test. The laboratory reactor achieved maximum TOC conversions close to 20 % (Run N6), whereas the solar system exhibited enhanced efficiency (up to 67.3 % conversion of TOC, Run S2).

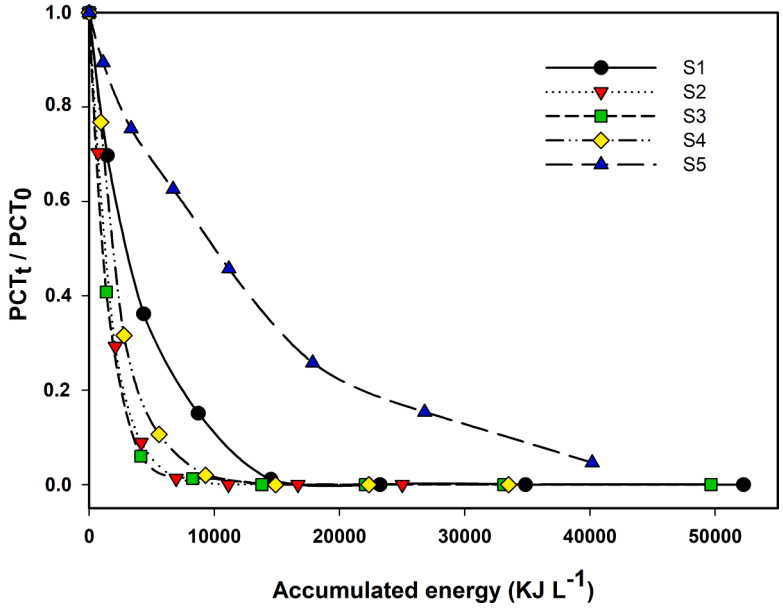

Fig. 3. Relative PCT concentration as a function of accumulated energy (Runs S1-S5) in the solar reactor experiments.

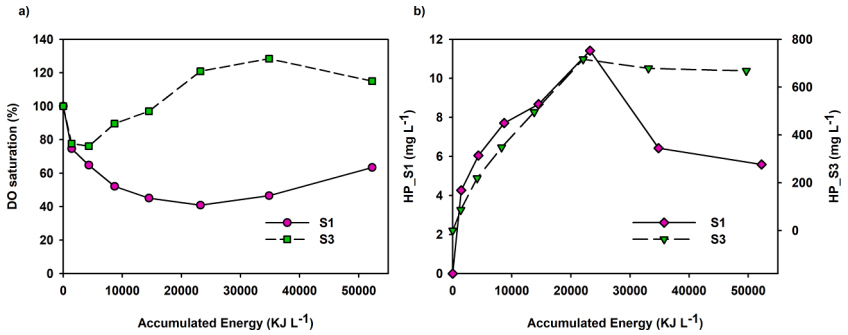

Fig. 4. Evolution of a) DO in percentage of saturation and b) HP concentration vs. accumulated energy.

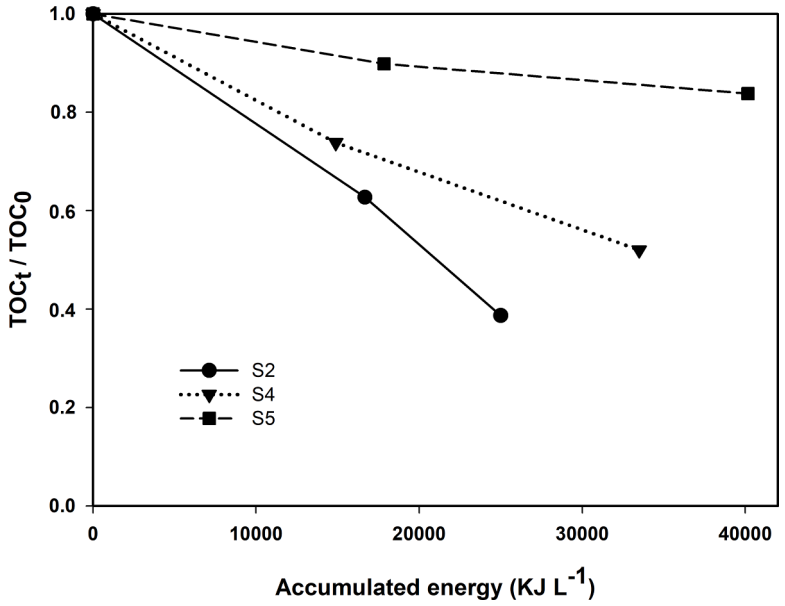

Fig. 5. Relative TOC concentration as a function of accumulated energy (Runs S2, S4 and S5) in the solar reactor experiments.

Finally, the toxicity in the system was evaluated considering the commonly proposed pathway for PCT photo-Fenton decomposition. This mechanism involves the direct attack of hydroxyl radicals on the PCT molecule, leading to the generation of acetamide and hydroquinone (HQ), which is subsequently oxidized to p-benzoquinone. These aromatic compounds undergo progressive transformation into non-aromatic molecules [21]. Fig. 6 depicts the changes in the percentage of inhibition of bioluminescence of *V. fischeri* bacteria after 15 min of incubation (*I(%)*), alongside the concentration of the formed HQ (the main reaction intermediate detected and quantified) as a function of the accumulated energy. This emphasizes that the observed toxicity mainly originates from HQ generated during PCT degradation.

In each case, the evolution of toxicity in the system was closely linked to the appearance and disappearance of HQ, reaching the maximum *I(%)* when the concentration of HQ in the reaction medium was the highest.

It's noteworthy that for the conditions depicted in Fig. 6a, a significant reduction in the toxicity of the system is observed after only 60 min of reaction (accumulated energy exceeding 1.10×10^4 KJ L^{-1}). Secondly, it can be seen that IW0.01 matrix did not represent a great addition of the initial toxicity to the system (Fig. 6b). However, a slight slowdown of the reaction was observed, since HQ disappeared at a higher accumulated energy than in the Run S1, which implied that the toxicity in the reaction medium also lasted longer. On the other hand, when the detergent was used at a concentration of 0.1 %, there was an extra addition on the initial toxicity of 23.71 % caused by only CIP300 at that quantity (blank test). Here, the presence of HQ at the end of the reaction, despite the great accumulated energy, caused that *I(%)* remained high (close to 60 %).

The HPLC chromatograms are shown in Fig. 7 for Runs S2 and S5, registered at 243 nm (wavelength used to quantify PCT). The disappearance of PCT can be seen (t_r= 7.29 min) and some peaks can be distinguished as reaction intermediates, of which only HQ was identified (t_r= 5.23 min). Here, the difference between working with ideal and real matrices is also noted. In the case of pure water, PCT and HQ were completely degraded at near 60 min of reaction, while in the simulated effluent there were still low quantities of both analytes at 180 min. Taking into account the low EC_{50} value of HQ (0.04 mg L^{-1}) for *V. fischeri* [49] and the presence of no identified peaks (between 1.5 and 3.3 min), it might be necessary to implement longer reaction times so as to completely reduce the toxicity when working with industrial wastewater.

4. Conclusions

This study highlights the crucial role of hydrogen peroxide dosing strategies in optimizing the ferrioxalate-assisted solar photo-Fenton process to remove Paracetamol. Through systematic analysis of various dosing methods, this research provides significant insights into their impact on pollutant removal efficiency, oxidant consumption, and toxicity levels across diverse water matrices.

The lab-scale reactor experiments highlighted the role of radiation

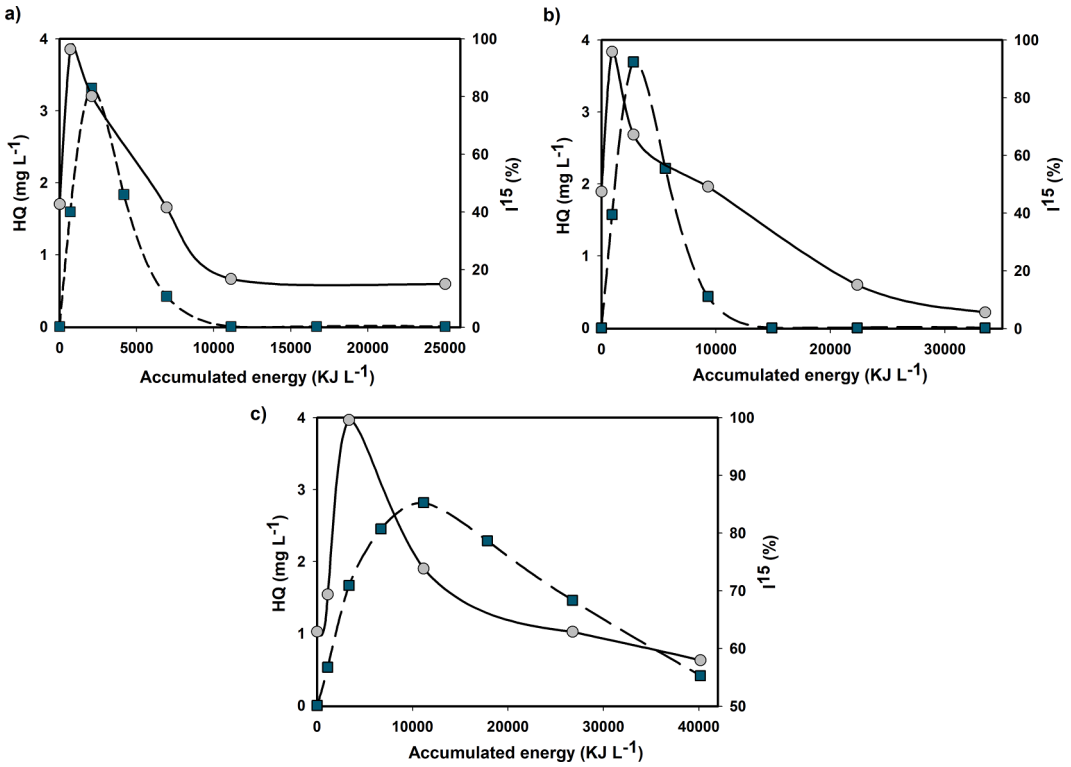

Fig. 6. Percentage of luminescence inhibition at 15 min (●) and HQ concentration (■) vs accumulated energy. a) Run S2 (UW); b) Run S4 (IW0.01) and c) Run S5 (IW0.1). HP= 378 mg L^{-1}.

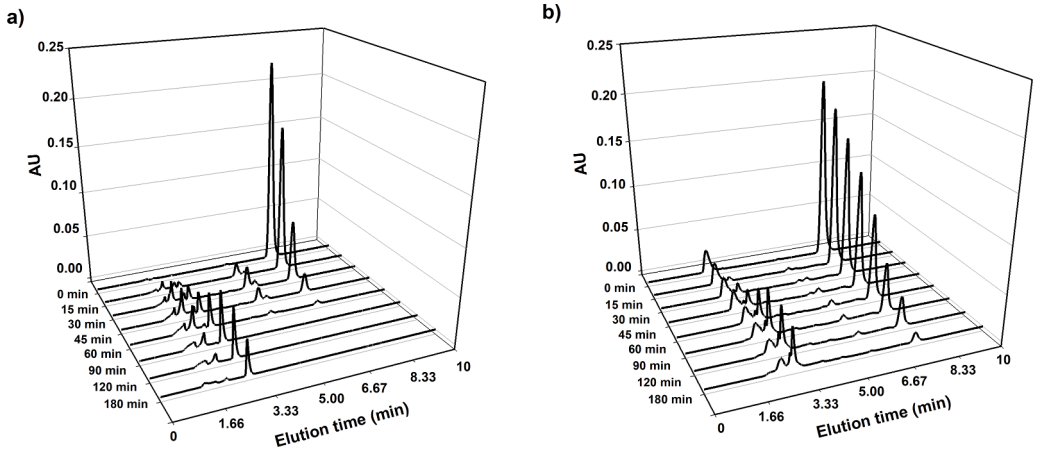

Fig. 7. HPLC chromatograms at 243 nm for solar experiments. a) Run S2 in ultrapure water; b) Run S5 in simulated industrial wastewater with 0.1 % CIP300. HP = 378 mg L^{-1}.

and the initial point dose of HP on the contaminant conversion efficiency. In particular, irradiation conditions significantly improved the process compared to dark conditions, with high conversion rates. However, excessive doses of HP led to unproductive consumption, which hindered the degradation of contaminants and generated unwanted reaction by-products.

The transition from lab-scale experiments to a pilot plant solar prototype demonstrated the scalability and effectiveness of the photodegradation process. Nonetheless, challenges emerged when confronting real industrial effluents, demanding extended reaction times to attain comparable conversion rates. The combined effect of UV/visible and thermal sunlight was able to almost completely degrade PCT after 180 min of reaction in the case of simulated industrial effluent treated in the solar reactor. However, the persistence of high toxicity levels (IW0.1 matrix) underscores the need for continued research on mitigation strategies for harmful by-products, such as hydroquinone, to ensure the environmental sustainability of wastewater treatment processes.

Overall, this comprehensive approach bridges the gap between laboratory findings and practical applications, providing valuable insights for the development of effective solutions to address pharmaceutical wastewater pollution. The robustness of the solar photo-Fenton process, even under conditions simulating industrial effluents, reaffirms its potential as a sustainable and scalable technology for wastewater treatment in pharmaceutical industries.

Funding

The authors are grateful to Universidad Nacional del Litoral (UNL, CAI+D 2020 50620190100040LI), Consejo Nacional de Investigaciones Científicas y Técnicas (CONICET, PIBAA 28720210100303CO, PIBAA 28720210100301CO and PIP11220210100060CO), and Secretaría de Ciencia, Tecnología e Innovación de la Provincia de Santa Fe (PEICID-2022-161) for financial support.

CRediT authorship contribution statement

Bárbara N. Giménez: Writing – review & editing, Writing – original draft, Visualization, Validation, Methodology, Investigation, Formal analysis, Conceptualization. **Agustina V. Schenone:** Writing – review & editing, Writing – original draft, Visualization, Validation, Supervision, Resources, Project administration, Methodology, Investigation, Funding acquisition, Formal analysis. **Leandro O. Conte:** Writing – review & editing, Writing – original draft, Visualization, Validation, Supervision, Resources, Project administration, Funding acquisition, Formal analysis, Conceptualization.

Declaration of competing interest

The authors declare that they have no known competing financial interests or personal relationships that could have appeared to influence the work reported in this paper.

Data availability

Data will be made available on request.

Acknowledgments

Bárbara N. Giménez particularly acknowledges to Consejo Nacional de Investigaciones Científicas y Técnicas (CONICET) for the PhD scholarship.

The authors are grateful to Universidad Nacional del Litoral (UNL, CAI+D 2020 50620190100040LI), Consejo Nacional de Investigaciones Científicas y Técnicas (CONICET, PIBAA 28720210100303CO, PIBAA 28720210100301CO and PIP11220210100060CO), and Secretaría de Ciencia, Tecnología e Innovación de la Provincia de Santa Fe (PEICID-2022-161) for financial support.

Supplementary materials

Supplementary material associated with this article can be found, in the online version, at doi:10.1016/j.ceja.2024.100627.

References

[1] J. Wang, L. Chu, L. Wojnárovits, E. Takács, Occurrence and fate of antibiotics, antibiotic resistant genes (ARGs) and antibiotic resistant bacteria (ARB) in municipal wastewater treatment plant: an overview, Sci. Total Environ. 744 (2020) 140997, https://doi.org/10.1016/J.SCITOTENV.2020.140997.

[2] P. Chaturvedi, P. Shukla, B.S. Giri, P. Chowdhary, R. Chandra, P. Gupta, A. Pandey, Prevalence and hazardous impact of pharmaceutical and personal care products and antibiotics in environment: a review on emerging contaminants, Environ. Res. 194 (2021) 110664, https://doi.org/10.1016/J.ENVRES.2020.110664.

[3] A. Ziylan-Yavas, D. Santos, E.M.M. Flores, N.H. Ince, Pharmaceuticals and personal care products (PPCPs): environmental and public health risks, Environ. Prog. Sustain. Energy. 41 (2022) e13821, https://doi.org/10.1002/EP.13821.

[4] R. Silori, V. Shrivastava, A. Singh, P. Sharma, M. Aouad, J. Mahlknecht, M. Kumar, Global groundwater vulnerability for Pharmaceutical and Personal care products (PPCPs): the scenario of second decade of 21st century, J. Environ. Manage. 320 (2022) 115703, https://doi.org/10.1016/J.JENVMAN.2022.115703.

[5] H.B. Hawash, A.A. Moneer, A.A. Galhoum, A.M. Elgarahy, W.A.A. Mohamed, M. Samy, H.R. El-Seedi, M.S. Gaballah, M.F. Mubarak, N.F. Attia, Occurrence and spatial distribution of pharmaceuticals and personal care products (PPCPs) in the aquatic environment, their characteristics, and adopted legislations, J. Water Process Eng. 52 (2023) 103490, https://doi.org/10.1016/J.JWPE.2023.103490.

[6] J.M. Peralta-Hernández, E. Brillas, A critical review over the removal of paracetamol (acetaminophen) from synthetic waters and real wastewaters by direct, hybrid catalytic, and sequential ozonation processes, Chemosphere 313 (2023) 137411, https://doi.org/10.1016/j.chemosphere.2022.137411.

[7] A. Ulvi, S. Aydın, M.E. Aydın, Fate of selected pharmaceuticals in hospital and municipal wastewater effluent: occurrence, removal, and environmental risk assessment, Environ. Sci. Pollut. Res. 29 (2022) 75609–75625, https://doi.org/10.1007/s11356-022-21131-y.

[8] E.S. Okeke, T.P.C. Ezeorba, C.O. Okoye, Y. Chen, G. Mao, W. Feng, X. Wu, Environmental and health impact of unrecovered API from pharmaceutical manufacturing wastes: a review of contemporary treatment, recycling and management strategies, Sustain. Chem. Pharm. 30 (2022) 100865, https://doi.org/10.1016/j.scp.2022.100865.

[9] E.M. Jiménez-Bambague, C.A. Madera-Parra, F. Machuca-Martinez, The occurrence of emerging compounds in real urban wastewater before and after the COVID-19 pandemic in Cali, Colombia, Curr. Opin. Environ. Sci. Heal. 33 (2023) 100457, https://doi.org/10.1016/j.coesh.2023.100457.

[10] X. Chen, L. Lei, S. Liu, J. Han, R. Li, J. Men, L. Li, L. Wei, Y. Sheng, L. Yang, B. Zhou, L. Zhu, Occurrence and risk assessment of pharmaceuticals and personal care products (PPCPs) against COVID-19 in lakes and WWTP-river-estuary system in Wuhan, China, Sci. Total Environ. 792 (2021) 148352, https://doi.org/10.1016/J.SCITOTENV.2021.148352.

[11] A. Jurado, E. Pujades, M. Walther, M.S. Diaz-Cruz, Occurrence, fate, and risk of the organic pollutants of the surface water watch List in European groundwaters: a review, Environ. Chem. Lett. 20 (2022) 3313–3333, https://doi.org/10.1007/s10311-022-01441-w.

[12] S.Y. Wee, N.A.H. Ismail, D.E.M. Haron, F.M. Yusoff, S.M. Praveena, A.Z. Aris, Pharmaceuticals, hormones, plasticizers, and pesticides in drinking water, J. Hazard. Mater. 424 (2022) 127327, https://doi.org/10.1016/J.JHAZMAT.2021.127327.

[13] M. Kumar, R. Silori, P. Mazumder, S.M. Tauseef, Screening of pharmaceutical and personal care products (PPCPs) along wastewater treatment system equipped with root zone treatment: a potential model for domestic waste leachate management, J. Environ. Manage. 335 (2023) 117494, https://doi.org/10.1016/J.JENVMAN.2023.117494.

[14] J. Liu, L. Duan, Q. Gao, Y. Zhao, F. Gao, Removal of typical PPCPs by reverse osmosis membranes: optimization of treatment process by factorial design, Membr. 13 (2023) 355, https://doi.org/10.3390/MEMBRANES13030355, 2023, Vol. 13, Page 355.

[15] T. Wang, J. He, J. Lu, Y. Zhou, Z. Wang, Y. Zhou, Adsorptive removal of PPCPs from aqueous solution using carbon-based composites: a review, Chinese Chem. Lett. 33 (2022) 3585–3593, https://doi.org/10.1016/J.CCLET.2021.09.029.

[16] A. Shah, A. Arjunan, A. Baroutaji, J. Zakharova, A review of physicochemical and biological contaminants in drinking water and their impacts on human health, Water Sci. Eng. 16 (2023) 333–344, https://doi.org/10.1016/J.WSE.2023.04.003.

[17] X. Chen, H. Rong, P. Ndagijimana, F. Nkinahamira, A. Kumar, D. Guo, B. Cui, Towards removal of PPCPs by advanced oxidation processes: a review, Results Eng. 20 (2023) 101496, https://doi.org/10.1016/j.rineng.2023.101496.

[18] S. Ziembowicz, M. Kida, Limitations and future directions of application of the Fenton-like process in micropollutants degradation in water and wastewater treatment: a critical review, Chemosphere 296 (2022) 134041, https://doi.org/10.1016/j.chemosphere.2022.134041.

[19] F. Machado, A.C.S.C. Teixeira, L.A.M. Ruotolo, Critical Review of Fenton and Photo-Fenton Wastewater Treatment Processes Over the Last Two Decades, Springer, Berlin Heidelberg, 2023, https://doi.org/10.1007/s13762-023-05015-3.

[20] L.O. Conte, A.V. Schenone, B.N. Giménez, O.M. Alfano, Photo-Fenton degradation of a herbicide (2,4-D) in groundwater for conditions of natural pH and presence of inorganic anions, J. Hazard. Mater. 372 (2019) 113–120, https://doi.org/10.1016/j.jhazmat.2018.04.013.

[21] B.N. Giménez, L.O. Conte, O.M. Alfano, A.V. Schenone, Paracetamol removal by photo-Fenton processes at near-neutral pH using a solar simulator: optimization by D-optimal experimental design and toxicity evaluation, J. Photochem. Photobiol. A Chem. 397 (2020) 112584, https://doi.org/10.1016/j.jphotochem.2020.112584.

[22] A. Gabet, H. Métivier, C. de Brauer, G. Mailhot, M. Brigante, Hydrogen peroxide and persulfate activation using UVA-UVB radiation: degradation of estrogenic compounds and application in sewage treatment plant waters, J. Hazard. Mater. 405 (2021) 124693, https://doi.org/10.1016/j.jhazmat.2020.124693.

[23] X. Yu, A. Cabrera-Reina, M. Graells, S. Miralles-Cuevas, M. Pérez-Moya, Towards an efficient generalization of the online dosage of hydrogen peroxide in photo-Fenton process to treat industrial wastewater, Int. J. Environ. Res. Public Health. 18 (2021) 13313, https://doi.org/10.3390/ijerph182413313.

[24] D. Rodríguez-García, P. Soriano-Molina, J.L. Guzmán Sánchez, J.L. García Sánchez, J.L. Casas López, J.A. Sánchez Pérez, A novel control system approach to enhance the efficiency of solar photo-Fenton microcontaminant removal in continuous flow raceway pond reactors, Chem. Eng. J. 455 (2023) 140760, https://doi.org/10.1016/j.cej.2022.140760.

[25] K. Nasr Esfahani, M. Pérez-Moya, M. Graells, Modelling of the photo-Fenton process with flexible hydrogen peroxide dosage: sensitivity analysis and experimental validation, Sci. Total Environ. 839 (2022), https://doi.org/10.1016/j.scitotenv.2022.155941.

[26] Y. Xiangwei, M. Graells, S. Miralles-Cuevas, A. Cabrera-Reina, M. Pérez-Moya, An improved hybrid strategy for online dosage of hydrogen peroxide in photo-Fenton processes, J. Environ. Chem. Eng. 9 (2021) 105235, https://doi.org/10.1016/j.jece.2021.105235.

[27] I. Oller, S. Malato, Photo-Fenton applied to the removal of pharmaceutical and other pollutants of emerging concern, Curr. Opin. Green Sustain. Chem. 29 (2021) 100458, https://doi.org/10.1016/j.cogsc.2021.100458.
[28] N.A. Khan, A.H. Khan, P. Tiwari, M. Zubair, M. Naushad, New insights into the integrated application of Fenton-based oxidation processes for the treatment of pharmaceutical wastewater, J. Water Process Eng. 44 (2021) 102440, https://doi.org/10.1016/J.JWPE.2021.102440.
[29] L.O. Conte, A.V. Schenone, O.M. Alfano, Ferrioxalate-assisted solar photo-Fenton degradation of a herbicide at pH conditions close to neutrality, Environ. Sci. Pollut. Res. 24 (2017) 6205–6212, https://doi.org/10.1007/s11356-016-6400-3.
[30] R.M.R. Santana, D.C. Napoleão, S.G. dos Santos Júnior, R.K.M. Gomes, N.F.S. de Moraes, L.E.M.C. Zaidan, D.R.M. Elihimas, G.E. do Nascimento, M.M.M.B. Duarte, Photo-Fenton process under sunlight irradiation for textile wastewater degradation: monitoring of residual hydrogen peroxide by spectrophotometric method and modeling artificial neural network models to predict treatment, Chem. Pap. 75 (2021) 2305–2316, https://doi.org/10.1007/s11696-020-01449-y.
[31] P. Soriano-Molina, S. Miralles-Cuevas, B. Esteban García, P. Plaza-Bolaños, J. A. Sánchez Pérez, Two strategies of solar photo-Fenton at neutral pH for the simultaneous disinfection and removal of contaminants of emerging concern. Comparative assessment in raceway pond reactors, Catal. Today. 361 (2021) 17–23, https://doi.org/10.1016/j.cattod.2019.11.028.
[32] P.B. Vilela, M.C. Maria, R.P. Mendonça Neto, F.A.R. de Souza, G.F.F. Pires, C. C. Amorim, Solar photo-Fenton mediated by alternative oxidants for MWWTP effluent quality improvement: impact on microbial community, priority pathogens and removal of antibiotic-resistant genes, Chem. Eng. J. 441 (2022) 136060, https://doi.org/10.1016/J.CEJ.2022.136060.
[33] E. Gualda-Alonso, P. Soriano-Molina, J.L. Casas López, J.L. García Sánchez, P. Plaza-Bolaños, A. Agüera, J.A. Sánchez Pérez, Large-scale raceway pond reactor for CEC removal from municipal WWTP effluents by solar photo-Fenton, Appl. Catal. B Environ. 319 (2022) 121908, https://doi.org/10.1016/J.APCATB.2022.121908.
[34] G. Lofrano, M. Faiella, M. Carotenuto, S. Murgolo, G. Mascolo, L. Pucci, L. Rizzo, Thirty contaminants of emerging concern identified in secondary treated hospital wastewater and their removal by solar Fenton (like) and sulphate radicals-based advanced oxidation processes, J. Environ. Chem. Eng. 9 (2021) 106614, https://doi.org/10.1016/j.jece.2021.106614.
[35] A. Durán, J.M. Monteagudo, I. San Martín, Operation costs of the solar photo-catalytic degradation of pharmaceuticals in water: a mini-review, Chemosphere 211 (2018) 482–488, https://doi.org/10.1016/j.chemosphere.2018.07.170.
[36] L.O. Conte, C.M. Dominguez, A. Checa-Fernandez, A. Santos, Vis LED Photo-Fenton degradation of 124-trichlorobenzene at a neutral pH using ferrioxalate as catalyst, Int. J. Environ. Res. Public Health. 19 (2022), https://doi.org/10.3390/ijerph19159733.
[37] L.I. Doumic, A.M. Ferro Orozco, M.A. Ayude, Fenton oxidation treatment of benzalkonium chlorides to prevent antibiotic resistance development in non-acclimated activated sludge system, J. Environ. Chem. Eng. 11 (2023) 111416, https://doi.org/10.1016/J.JECE.2023.111416.
[38] G.D. Silva, E.O. Marson, L.L. Batista, C. Ueira-Vieira, M.C.V.M. Starling, A. G. Trovó, Contrasting the performance of photo-Fenton at neutral pH in the presence of different organic iron-complexes using hydrogen peroxide or persulfate as oxidants for naproxen degradation and removal of antimicrobial activity, Process Saf. Environ. Prot. 147 (2021) 798–807, https://doi.org/10.1016/j.psep.2021.01.005.
[39] M. Pacheco-Álvarez, R. Picos Benítez, O.M. Rodríguez-Narváez, E. Brillas, J. M. Peralta-Hernández, A critical review on paracetamol removal from different aqueous matrices by Fenton and Fenton-based processes, and their combined methods, Chemosphere 303 (2022) 134883, https://doi.org/10.1016/j.chemosphere.2022.134883.
[40] B.N. Giménez, L.O. Conte, S.A. Duarte, A.V. Schenone, Improvement of ferrioxalate assisted Fenton and photo-Fenton processes for paracetamol degradation by hydrogen peroxide dosage, Environ. Sci. Pollut. Res. 31 (2024) 13489–13500, https://doi.org/10.1007/s11356-024-32056-z.
[41] B.N. Giménez, A.V. Schenone, O.M. Alfano, L.O. Conte, Reaction kinetics formulation with explicit radiation absorption effects of the photo-Fenton degradation of paracetamol under natural pH conditions, Environ. Sci. Pollut. Res. 28 (2021) 23946–23957, https://doi.org/10.1007/s11356-020-11993-5.
[42] G. Dalgic, F.I. Turkdogan, K. Yetilmezsoy, E. Kocak, Treatment of real paracetamol, Chem. Ind. Chem. Eng. Q. 23 (2017) 177–186.
[43] Resolución n° 1089/82, Reglamento para el control del vertimiento de líquidos residuales. Dirección Provincial de Obras Sanitarias. Provincia de Santa Fe., (1982). http://www.santafe.gov.ar/index.php/web/content/download/22767/111069/file/ResoluciónNo1089-82.pdf (accessed July 4, 2024).
[44] F. Audino, L.O. Conte, A.V. Schenone, M. Pérez-Moya, M. Graells, O.M. Alfano, A kinetic study for the Fenton and photo-Fenton paracetamol degradation in an annular photoreactor, Environ. Sci. Pollut. Res. 26 (2019) 4312–4323, https://doi.org/10.1007/s11356-018-3098-4.
[45] E. Ono, M. Tokumura, Y. Kawase, Photo-Fenton degradation of non-ionic surfactant and its mixture with cationic or anionic surfactant, J. Environ. Sci. Heal. Part A. 47 (2012) 1087–1095, https://doi.org/10.1080/10934529.2012.668034.
[46] M.C.V.M. Starling, P.H.R. dos Santos, F.A.R. de Souza, S.C. Oliveira, M.M.D. Leão, C.C. Amorim, Application of solar photo-Fenton toward toxicity removal and textile wastewater reuse, Environ. Sci. Pollut. Res. 24 (2017) 12515–12528, https://doi.org/10.1007/s11356-016-7395-5.
[47] L.O. Conte, P. Querini, E.D. Albizzati, O.M. Alfano, Photonic and quantum efficiencies for the homogeneous photo-Fenton degradation of herbicide 2,4-D using different iron complexes, J. Chem. Technol. Biotechnol. 89 (2014) 1967–1974, https://doi.org/10.1002/jctb.4284.
[48] R. Poblete, J. Bakit, Technical and economical assessment of the treatment of vinasse from Pisco production using the advanced oxidation process, Environ. Sci. Pollut. Res. 30 (2023) 70213–70228, https://doi.org/10.1007/s11356-023-27390-7.
[49] A. Santos, P. Yustos, A. Quintanilla, F. García-Ochoa, J.A. Casas, J.J. Rodríguez, Evolution of toxicity upon wet catalytic oxidation of phenol, Environ. Sci. Technol. 38 (2004) 133–138, https://doi.org/10.1021/es030476t.